Celal Bayar University Journal of Science
Volume 15, Issue 1, 2019, p 57-64
Doi: 10.18466/cbayarfbe.459295

The Semi-Empirical Determination of K_α X-ray, KLL Auger Line and L subshell level widths for 3d transition elements at 59.5 keV

Kadriye Kundeyi[1], **Nuray Kup Aylikci**[2*]

[1]Metallurgical and Material Engineering, Faculty of Natural Sciences and Engineering, Iskenderun Technical University, Iskenderun, Hatay, Turkey
[2]Energy Systems Engineering, Faculty of Natural Sciences and Engineering, Iskenderun Technical University, Iskenderun, Hatay, Turkey
[*]nuray.aylikci@iste.edu.tr

Received: 12 September 2018
Accepted: 08 February 2019
DOI: 10.18466/cbayarfbe.459295

Abstract

The emission of X-rays in K_α and KLL Auger energy regions were analyzed for transition metals by using energy dispersive X-ray fluorescence (EDXRF) system. To acquire more information in this energy region, the semi-empirical determination of K_α, Auger line-widths and the L sub-shell level widths were performed. Since K shell is a core shell for transition metals and it is not easily be affected by valence shell electronic distributions, K shell fluorescence yields were used for the semi-empirical determinations. In the experiment, elemental form of transition metals were excited by 59.5 keV γ-rays from ^{241}Am annular source and the emitted X-ray photons were counted by Ultra-LEGe detector with a resolution of 150 eV at 5.9 keV. The obtained results were compared with the other studies in the literature.

Keywords: 3d transition metals; EDXRF; K_α line-width; KLL Auger line-width; L subshell level-width**.**

1. Introduction

Transition metals are an essential factor for technological devices and these metals have many applications in optoelectronic materials, sensors, shape memory alloys and etc. And it is not possible to produce any material without characterization by different methods. For instance, X-ray diffraction experiment requires the analytical description of main X-ray emission lines for rocking curve and line profile analysis. The X-ray emissions are not only helpful in X-ray diffraction analysis but also in X-ray elemental characterisation which is important in material science. X-ray spectroscopic techniques is the most powerful and sophisticated approaches for the investigation of electronic structure and properties of solids [1].

The various applications of 3d transition metals in different technological areas are due to the valence shell electronic distribution which defined as $3d^n4s^m$. Different n and m values cause to obtain various spectroscopic values for each configuration. The transition metal atoms are connected to each other by metallic bond to form a metallic structure. In metallic bonds, the electrons are free to move throughout the structure and valence electrons are loosely connected to the valence shell. In spectroscopic phenomena, radiative and radiationless transitions are conversely proportional to each other since probability of these phenomena is equal to 1. Also, Auger transitions are more probable than X-ray transitions where the binding energies of electrons decrease. And so, it can be concluded that, the probability of radiative and radiationless transitions are conversely proportional to each other.

Auger effect is an important decay for explaining the surface structure of any metal by using chemical shift measurements and qualitative analysis of trace elements on surfaces [2]. KLL and KMM Auger spectra and the respective Auger parameters of V, Cr, Mn and Fe were reported by using high resolution measurements where the elemental form of elements prepared as thin metallic layers. The significant deviations in the obtained values were attributed to the surface chemical state of the samples, the spectrum evaluation method and the differences in Auger transition process following electron capture or photoionization [3]. It is known that the diagram lines in X-ray emission spectrum are corresponds to one hole transition to the upper state where one electron is removed from an inner shell. The satellite lines or non-diagram lines are usually appeared at the lower or higher side of the main lines in 3d transition metals. These lines are created by the multiple ionizations since 3d transition metals can occur in different oxidation states. The non-diagram line contributions in the $K_{\beta1,3}$ X-ray spectra of 3d transition metals were measured by high resolution spectrometry. $K_{\beta'}$, $K_{\beta5}$ and KMM lines were defined as second order radiative contributions and it was found a correlation between the oxidation states of chromium and the second order radiative contributions [4]. The asymmetry indices, KM shake probabilities and $K_{\alpha1,2}$ X-ray line widths were investigated within Berger's two-Lorentzian functions model by using double crystal spectrometer. It was found that the shake-off satellite lines appeared between the $K_{\alpha1}$ and $K_{\alpha2}$ lines and the asymmetry index of $K_{\alpha1}$ in 3d transition metals were ascribed to the 3d spectator hole [5]. $K_{\alpha1,2}$ and $K_{\beta1,3}$ X-ray spectra of 3d transition metals were investigated and Z dependent trends were reported [6]. $K_{\alpha1,2}$ X-ray spectra in 3d transition elements were reported and it was concluded that FWHM of $K_{\alpha1}$ line increased from Ti to Zn as compared other theoretical values but on the contrary, different tendency was observed for $K_{\alpha2}$ lines between Co and Ni where the lines had a maximum and then decreased to Zn [7]. $K_{\alpha1,2}$ and $K_{\beta1,3}$ X-ray spectra of copper which defined as iron group metal [8], $K_{\alpha1,2}$ X-ray spectra of Cr, Fe, Co, Ni and Cu [9], the structural trends in K_{α} spectral profiles from Z=21 to Z=25 [10], the reconstruction of K_{α} spectra for titanium using only instrumental broadening widths and the investigation of shake process for transition metals [11]. Apart from these studies, $K_{\beta1,3}$ X-ray spectra for elements from Ca to Ge [12] and from Mg to Zn [13] were inspected by high resolution and wavelength dispersive measurements respectively. And finally Auger electron spectra of Cr, Mn, Fe, Co and Ni metals and their oxides were reported for the energy range between 0 to 100 eV. At low energies (0-30 eV), the extra lines were detected which could not be explained by electron transitions in isolated atoms besides the Auger spectra for transition metal oxides [14]. These studies in the literature generate valuable data for the development of theoretical estimations for understanding the shell structure of transitions metals that the transitions are dominated by Auger process. According to the literature survey given above, different experimental and theoretical methods were used for the X-ray and Auger line widths. It is known that the equipment which determines the KLL Auger and other radiative X-ray lines with higher sensitivity is very expensive. But the calculations can be easily performed by using energy dispersive X-ray fluorescence measurements. The K_{α} spectrum cannot be resolved as $K_{\alpha1}$ and $K_{\alpha2}$ lines and each Auger lines are combined in a one spectrum as KLL. K_{β} (transitions from M shell to K) lines are not studied since the transitions will be easily affected by valence shell electronic distributions. To overcome spectral resolution, only K shell fluorescence yields were used since K shell is the innermost level for all elements in the periodic table and is unique. In this study, the parameters for elemental 3d transition metals were determined semi-empirically by using K shell fluorescence yield that explained in Materials and Methods section. These semi-empirically determination of level and line widths will be the first by using EDXRF at 59.5 keV even if the peaks $K_{\alpha1}$, $K_{\alpha2}$ X-ray and KLL Auger lines are not resolved by studied system. We believe that the obtained measurements will supply more data for theoretical estimations for understanding complex shell structure of 3d transition metals.

2. Materials and Methods

2.1. Experimental Measurements

The elemental forms of 3d transition metals were obtained commercially (Sigma-Aldirich) and the purity of the materials was better than 99.998%. Powder samples were sieved using 400 mesh and the particle sizes were so sufficiently small that there was no significant correction to the data. After that, the pure samples were prepared by supporting on a mylar film of 2.847 mg/cm^2 thickness. Pure samples were irradiated by ^{241}Am annular radioactive source at 59.5 keV. The experimental set-up was arranged as in our previous paper [15] *but the measurements were repeated to obtain new updated photo-peaks*. The obtained photo-peaks were used for determining the K X-ray production cross-sections and other fluorescence parameters.

2.1.1. Peak evaluation process

The obtained spectra were plotted by using Origin Company software program (Origin 7.5 demo version) and the fitting procedure was performed by least-squares. A least squares fitting method was chosen since the spectral deconvolution was the main problem due to the strong peak overlapping in EDXRF systems. For this reason, good statistics will be essential for the accurate peak areas. In this paper, the values of χ_{υ}^2 for K X-ray peaks between 0.79-0.87 respectively. The higher values of R^2 mean that the model suits data better. The R^2 is 0.99946-0.99987. The value 0.99987 means that 99.987% of the variance in Y is predictable from X. This means that the fits are fairly well-defined. Figure 1 shows the K_{α} and K_{β} X-ray peaks for elemental Fe with residue spectra. The residue spectrum deals with the peak investigating process. If it is found out to the hidden peak or peaks, the residue spectrum has to be investigated carefully.

In this study, the areas of the analyzed K X-ray peaks were used for the determination of K X-ray production cross-sections of 3d transition elements.

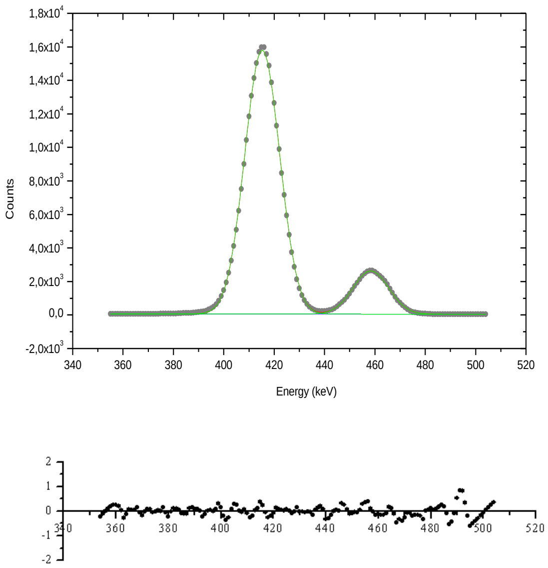

Figure 1. The K X-ray spectra of elemental Fe with residue spectrum.

2.1.2. The determination of fluorescence parameters

The K_α and K_β X-ray production cross-sections were determined by using the following equations;

$$\sigma_{Ki} = \frac{A}{N} \frac{N_{Ki}}{I_0 G \varepsilon_{Ki} \beta_{Ki} m_i} \text{ (i= α, β) [16]} \qquad \textbf{(2.1)}$$

where A is atomic weight of studied elements, N is Avogadro constant, N_{Ki} is area under the photo-peak corresponding to the K_i x rays, I_0 is the intensity of the incident radiation, G is the geometric factor, ε_{Ki} is the detection efficiency for the K_i X-rays, β_{Ki} is the self-absorption correction factor for the target material and finally m_i is the thickness of the target in g/cm^2.

The self-absorption correction factors for elements were determined with the same relation as explained in our previous study [15]. The detection efficiency of EDXRF system means to the ratio of the number of particles detected per unit time to the number of particles impinging upon the detector per unit time. In this study, $I_0G\varepsilon$ values were determined for different energies and the obtained values were plotted as a function of energy. From the fitting procedure two polynomial equations were obtained as written below.

$$Y = A + B_1X + B_2X^2 + B_3X^3 \text{ (part I) [22]} \qquad \textbf{(2.2)}$$

$$Y = C + D_1X + D_2X^2 \text{ (part II) [22]} \qquad \textbf{(2.3)}$$

Figure 2 shows the detector efficiency plot as a function of energy after fitting process.

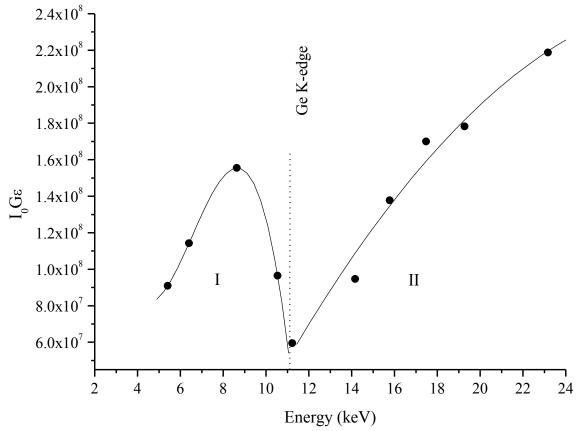

Figure 2. The plot of detector efficiency versus energy

Using K X-ray production cross-section values, K shell fluorescence yields were determined as written below,

$$\omega_K = \frac{\sigma_{K\alpha} + \sigma_{K\beta}}{\sigma_K^p(E)} \text{ [22]} \qquad \textbf{(2.4)}$$

In this relation σ_{K_α} and σ_{K_β} are the K_α and K_β X-ray production cross-sections which are obtained from the photo-peak areas from the new measurements respectively. The photoionization cross-section at 59.5 keV is denoted as $\sigma_K^p(E)$ and taken from Ref. [18].

It is known that the principal quantum numbers specify the shell structure of the atom and each shell determines the energy which called as K, L, M, N, O and etc. Each shell splits off subshell except for K shell. The valence states for 3d transition elements correspond to the M and upper subshells and the electronic configuration can easily be change for 3d transition metals since each element can take more than one valence state. Since the outer shell can rearrange between each other, the obtained shape of photo-peaks will be asymmetric. And also, the measured parameters can take different values according to the valence electronic configuration. Any changes in 3d4s states can easily affect the lower 3s3p states where M shell is open. The other point to note is the semi-empirical determination of $K_{\alpha1}$ and $K_{\alpha2}$ and KLL Auger line widths of pure elements between Z=21 and Z=30 despite the low resolution of Ultra LEGe detector to separate K_α and KLL Auger lines. Using the K shell fluorescence yields of 3d transition metals, K shell level width is determined by the following equation,

$$\Gamma_K = \frac{\Gamma_K(R)}{\omega_K} \text{ [19]} \qquad \textbf{(2.5)}$$

where total rate of K X-ray emission is denoted as $\Gamma_K(R)$[18] and K shell fluorescence yield is ω_K. The semi-empirical K_α line widths were calculated as a sum of levels involved to the transitions,

$$\Gamma_{K_{\alpha_1}} = \Gamma_{L_3} + \Gamma_K \,[19] \quad \textbf{(2.6)}$$

$$\Gamma_{K_{\alpha_2}} = \Gamma_{L_2} + \Gamma_K \,[19] \quad \textbf{(2.7)}$$

where $\Gamma_{K_{\alpha1}}$ and $\Gamma_{K_{\alpha2}}$ determine the line widths of K_α X-ray lines. K shell level widths (Γ_K) are determined in the context of this study and finally, L subshell level widths (except L_1) are denoted as Γ_{L_2} and Γ_{L_3} and these values are taken from the study of Krause and Oliver [19].

It is known that the asymmetric shape of the photo-peaks of 3d transition metals is partially due to the fact that the valence electrons can move easily throughout the crystal structure. The determining of Auger line widths are important for the understanding of the treatment of wave functions of outer shell electrons since they are responsible for the constituting any chemical materials which are useful for technological devices. These obtained values are important for both of the elemental analysis of any material and the theoretical estimations of atomic shell structure. And for these reasons the Auger line widths of KLL are obtained by the similar way as follows.

$$\Gamma_{KLL} = \Gamma_K + \Gamma_{L_k} + \Gamma_{L_l} \,[19] \quad \textbf{(2.8)}$$

In this relation, K shell level widths for 3d elements are determined by Eq. 2.3 and other values of L subshell level widths are taken from Krause and Oliver's study [19]. For the empirical determination of subshell level widths, calculated K X-ray line widths ($\Gamma_{K_{\alpha1}}$,$\Gamma_{K_{\alpha2}}$ and $\Gamma_{K_{\alpha3}}$) are used in the literature which are taken from the Ref.[20]. If the Eqs. 2.4 and 2.5 are rearranged again, they can be written,

$$\Gamma_{L_3} = \Gamma_{K_{\alpha_1}} - \Gamma_K \quad \textbf{(2.9)}$$

$$\Gamma_{L_2} = \Gamma_{K_{\alpha2}} - \Gamma_K \quad \textbf{(2.10)}$$

$$\Gamma_{L_1} = \Gamma_{K_{\alpha_3}} - \Gamma_K \quad \textbf{(2.11)}$$

In this relation, Γ_K values are the obtained values in this study. The experimental procedures are the same as in our previous study [15] and the measurements are repeated again at 59.5 keV using Ultra LEGe to obtain new updated semi-empirical values.

The uncertainties in the measurements are estimated to be less than 6% and are found propagating the errors in various parameters used for determination of X-ray parameters. The uncertainties in these parameters are listed in Table 1and the quadrature sums of uncertainties determine the calculated error value.

Table 1. Uncertainties in the quantities used to determine the parameters.

Quality	Nature of uncertainty	Uncertainty (%)
$N(K_i)$ (i=α, β, KLM, KMM)	Counting statistic	≤ 3
$I_0G\varepsilon_{K_1}$	Errors in different parameters used to evaluate factor	≤ 2
β	Error in the absorption coefficients at incident and emitted photon energies	≤ 3
t	Non-uniform thickness	≤ 2

3. Results and Discussion

The obtained values of the K shell fluorescence yields; K shell and L sub-shell level widths, KLL Auger and K_α X-ray line widths were shown between Tables 2–5. First, K shell fluorescence yields were determined using Eq. 2.4 and the measurements were repeated at 59.5 keV which were different from our previous study [15]. Using the ratio of the total radiative transition rates and K shell fluorescence yield values (Eq. 2.5), K shell level widths were obtained for 3d transition elements.

It can be seen from Table 2 that the K shell level widths are more consistent with the results of Ref. [20]. When the results are compared with Krause and Oliver's study [19], it can be seen that the obtained values are 13% compatible for Sc, 11% for Ti, Mn and Fe, 12% for V and Cr, 10% for Co, Ni, Cu and finally 8% for Zn. Also it can be seen that the compatibility ratio changes between 10% and 5% from Sc to Zn compared to the results of Campbell and Papp [21].

Table 2. K shell fluorescence yields and K shell level widths of 3d transition elements.

Z	Element	ω_K	Γ_K	Γ_K[19]	Γ_K[20]	Γ_K[21]
21	Sc	0.2011±0.0102	0.7459±0.0380	0.86	0.80	0.83
22	Ti	0.2224±0.0113	0.8363±0.0426	0.94	0.86	0.89
23	V	0.2556±0.0130	0.8920±0.0455	1.01	0.92	0.96
24	Cr	0.2897±0.0147	0.9531±0.0486	1.08	0.99	1.02
25	Mn	0.3240±0.0165	1.0278±0.0524	1.16	1.07	1.11
26	Fe	0.3567±0.0182	1.1102±0.0566	1.25	1.15	1.19
27	Co	0.3907±0.0199	1.2004±0.0612	1.33	1.24	1.28
28	Ni	0.4238±0.0216	1.3001±0.0663	1.44	1.33	1.39
29	Cu	0.4633±0.0236	1.3879±0.0707	1.55	1.44	1.49
30	Zn	0.4838±0.0246	1.5440±0.0787	1.67	1.56	1.62

Table 3 presents the performed results of L sub shell level widths and it can be seen that the results are more compatible with the results of Ref.[20]. The other remarkable point is that the compatibility ratio (the percentage difference between the obtained and the other values in the literature) decreases with the increment of atomic number from Sc to Zn.

The obtained results from Table 3 are not consistent with the semi-empirical values of Krause and Oliver [19]. This is an expected result since the semi-empirical determinations for K and L sub-shell are generally performed by using a relation similar to Eq.2.5. But in this study, a different method has been tried (Eqs. 2.9, 2.10 and 2.11).

Table 3. L subshell level widths of 3d transition elements.

Z	Element	Γ_{L1}	Γ_{L1} [19]	Γ_{L1} [20]	Γ_{L1} [21]	Γ_{L2}	Γ_{L2} [19]	Γ_{L2} [20]	Γ_{L2} [21]	Γ_{L3}	Γ_{L3} [19]	Γ_{L3} [20]	Γ_{L3} [21]
21	Sc	4.6441±0.2368	2.21	4.59	3.30	0.2841±0.0144	0.19	0.23	0.36	0.2841±0.0144	0.19	0.23	0.23
22	Ti	5.2937±0.2699	2.34	5.27	3.9	0.2737±0.0139	0.24	0.25	0.52	0.2737±0.0139	0.22	0.25	0.25
23	V	5.8980±0.3007	2.41	5.92	4.60	0.3080±0.0157	0.26	0.28	0.78	0.3080±0.0157	0.24	0.28	0.28
24	Cr	6.8569±0.3497	2.54	6.83	5.20	0.3469±0.0177	0.29	0.32	0.76	0.3569±0.0182	0.27	0.32	0.32
25	Mn	6.7622±0.3448	2.62	6.72	6.20	0.3922±0.0200	0.34	0.36	0.97	0.4022±0.0205	0.32	0.36	0.36
26	Fe	7.4198±0.3784	2.76	7.38	7.05	0.4398±0.0224	0.37	0.40	1.14	0.4498±0.0229	0.36	0.41	0.41
27	Co	8.0096±0.4084	2.79	7.97	7.20	0.4896±0.0249	0.43	0.46	1.13	0.4996±0.0254	0.43	0.47	0.47
28	Ni	8.5499±0.4360	2.89	8.51	6.40	0.5599±0.0285	0.52	0.53	0.98	0.5599±0.0285	0.48	0.53	0.53
29	Cu	9.1821±0.4682	3.06	9.13	5.50	0.6521±0.0332	0.62	0.60	1.04	0.6621±0.0337	0.56	0.61	0.61
30	Zn	9.5160±0.4853	3.28	9.50	4.80	0.6860±0.0349	0.72	0.67	1.06	0.6960±0.0354	0.65	0.68	0.68

The semi-empirical determinations were achieved by Krause and Oliver [19] using the Scofield's radiative transition rates and Krause's fluorescence yields evaluation. But in this study, K_α X-ray line widths are taken from Perkins's study and the obtained K shell level-widths are extracted from the taken values. And so it can be said that different approximations of different theoretical studies influence the tabulated results. Because, the results were only consistent with the Perkin's result [20] where the K_α X-ray line widths were taken. The determination of these parameters are model dependent and can take different values according to the different theoretical approximations. Because of this reason, more experimental and new theoretical values should be obtained. If the K_α X-ray line widths were taken from other studies (such as Refs [19] and [21]) the results would be consistent with the results of Refs. [19] and [21]. KLL Auger and K_α X-ray line widths are tabulated as Tables 4 and 5. According to Table 4, KL_1L_1 and KL_1L_2Auger line widths are in agreement with the other values in the literature where the change percent is within experimental error limits.

Celal Bayar University Journal of Science
Volume 15, Issue 1, 2019, p 57-64
Doi: 10.18466/cbayarfbe.459295

Table 4. KLL Auger line widths of 3d transition elements.

Z	Element	Γ_{KL1L1}	Γ_{KL1L1} [19]	Γ_{KL1L2}	Γ_{KL1L2} [19]	Γ_{KL2L3}	Γ_{KL2L3} [19]
21	Sc	5.1659±0.2634	5.27	3.1459±0.1604	3.26	1.1259±0.0574	1.25
22	Ti	5.5163±0.2813	5.62	3.4163±0.1742	3.52	1.2963±0.6661	1.40
23	V	5.7120±0.2913	5.84	3.5620±0.1816	3.69	1.3920±0.0709	1.52
24	Cr	6.0331±0.3076	6.15	3.7831±0.1929	3.90	1.5131±0.0771	1.64
25	Mn	6.2678±0.3196	6.40	3.9878±0.2033	4.12	1.6878±0.0860	1.82
26	Fe	6.6302±0.3381	6.77	4.2402±0.2162	4.38	1.8402±0.0938	1.99
27	Co	6.7804±0.3458	6.91	4.4204±0.2254	4.56	2.0604±0.1050	2.19
28	Ni	7.0801±0.3610	7.22	4.7101±0.2402	4.85	2.3001±0.1173	2.44
29	Cu	7.5079±0.3829	7.67	5.0679±0.2584	5.23	2.5679±0.1309	2.73
30	Zn	8.1040±0.4133	8.22	5.5440±0.2827	5.66	2.9140±0.1486	3.04

Contrary to these results, KL_2L_3 Auger widths change beyond of experimental error limits (6%–7%) for Sc, V, Cr and Fe.

The same trends will be observable for $K_{\alpha 1}$ and $K_{\alpha 2}$ line widths which can be seen in Table 5. The change percent ratio of the obtained values to the literature is beyond of the experimental error limits except for Co, Cu and Zn when the calculated values of Krause and Oliver are concerned [19]. Also, $K_{\alpha 2}$ line widths are in agreement with the values of Krause and Oliver from Co to Zn. The other remarkable point is that the best agreement is achieved by comparing the values with Ref. [20].

Table 5. K_α X-ray line widths of 3d transition elements.

Z	Element	$\Gamma_{K\alpha 1}$	$\Gamma_{K\alpha 1}$ [19]	$\Gamma_{K\alpha 1}$ [20]	$\Gamma_{K\alpha 2}$	$\Gamma_{K\alpha 2}$ [19]	$\Gamma_{K\alpha 1}$ [20]
21	Sc	0.9359±0.0477	1.05	1.03	0.9359±0.0477	1.06	1.03
22	Ti	1.0563±0.0538	1.16	1.11	1.0763±0.0549	1.18	1.11
23	V	1.1320±0.0577	1.26	1.20	1.1520±0.0587	1.28	1.20
24	Cr	1.2231±0.0623	1.35	1.31	1.2431±0.0633	1.37	1.30
25	Mn	1.3478±0.0687	1.48	1.43	1.3678±0.0697	1.50	1.42
26	Fe	1.4702±0.0749	1.61	1.56	1.4802±0.0754	1.62	1.55
27	Co	1.6304±0.0831	1.76	1.70	1.6304±0.0831	1.76	1.69
28	Ni	1.7801±0.0907	1.94	1.86	1.8201±0.0928	1.96	1.86
29	Cu	1.9479±0.0993	2.11	2.05	2.0079±0.1024	2.17	2.04
30	Zn	2.1940±0.1119	2.32	2.24	2.2640±0.1154	2.39	2.23

For the semi-empirical determination of studied parameters K shell fluorescence yields are utilized since K shell is close to the atomic nucleus and it is not separated into the sub-shells. Also K shell is the innermost shell for all of the atoms in periodic table and so it cannot be easily affected by valence electronic structure change except for elements with low atomic number and the changes in the innermost K shell cannot be determined since the changes will be inside experimental error limits. But the radiative K X-ray transitions can be affected by the outer shell electronic distributions. In our previous studies, it was obtained that K shell fluorescence yields did not change by the outer shell electronic distributions in energy dispersive x-ray fluorescence systems [22-23]. For the L subshell level widths determination, K_α line (originates from the transitions between L and K shell) widths are used in the literature [20] since these lines cannot be affected by outermost shell electronic distributions in 3d metals where the valence electrons are free to move throughout the metallic structure.

It is known that, the semi-empirically obtained natural line and level widths in this study are different from the actual widths in an experiment and other values in the literature due to the several broadening effects. These broadening effects (such as multiple splitting, multiple ionization) are in general small except for light elements. Also, other broadening effects should be considered such as instrumental effect due to the experimental set-up, solid state effect and etc.

The biggest compatibility ratio is achieved for Sc for all measurements. The reason of this result may be the open shell structure of Sc element. The valence electrons belonging to the unfilled M sub-shell may be

Celal Bayar University Journal of Science
Volume 15, Issue 1, 2019, p 57-64
Doi: 10.18466/cbayarfbe.459295

move easily to the outermost levels. This means that the binding energy of valence electrons will decrease and the obtained natural width may be different from the atomic state of Sc. This assumption is confirmed by the results of Zn element. The obtained results are more consistent for Zn element compared to the other calculations. The reason of this may be due to d orbital is completely filled.

And finally, it should be note to the transitions of Coster-Kronig type which are energetically possible and dominant in the region Z≤30. Especially $L_1L_3M_x$ (x=1,2,3), $L_2L_3M_y$ (y=4,5) and $M_1M_2M_y$ (y=4,5) transition can affect the obtained results for Auger and line widths [24]. This fact may be the reason of the incompatible results for X-ray and Auger line widths for some 3d transition metals.

These obtained values are important data for the scientific investigations in different areas such as material science where XRF analysis is used for the determination of elemental composition or XRD analysis for the determination of the crystal structure of any material which affects the physical/chemical properties of the specimens worked. On the other hand, these performed values supply more data for the theoretical estimations of atomic shell structure calculations and this study is the first for the semi-empirical determination of K shell and L subshell level widths, KLL Auger and K_α X-ray line widths at 59.5 keV by EDXRF method even though the Auger and X-ray peaks are not well separated due to the low resolution of detector system. To overcome this problem, K shell fluorescence yields are used and semi-empirical determinations are performed. For the future studies, the measurements should be repeated at different energies by using different methods.

4. Conclusion

In this study K shell and L subshell level widths, K_α X-ray line and KLL Auger line widths were determined at 59.5 keV by using energy dispersive X-ray fluorescence analysis. The interesting results were obtained by comparing with other values in the literature and especially the incompatible results for line widths were attributed to the Auger transitions of Coster-Kronig type.

Finally, it has been believed that this study will be a guide for future studies in the case of theoretical estimations of atomic structure calculations.

Acknowledgement

I gratefully acknowledge to Prof. Dr. Engin Tirasoglu for his valuable contribution in the period of my academic career.

Author’s Contributions

Kadriye Kundeyi: Assisted the experiment and result analysis.

Nuray Kup Aylikci: Managed in analytical analysis on the structure, supervised the experiment’s progress, result interpretation and helped in manuscript preparation and writing.

Ethics

There are no ethical issues after the publication of this manuscript.

References

1. Neumann, M, Kuepper, K. 2009. X-ray spectroscopic techniques are powerful tools for electronic structure investigations of transition metal oxides. *Surface Science;* 603: 1613–1621.

2. Haas, T.W, Grant, J.T, Dooley G.J. 1970. Auger electron spectroscopy of transition metals. *Physical Review B*; 1: 1449–1459.

3. Nemethy, A, Köver, L, Cserny, I, Varga, D, Barna P.B. 1996. The KLL and KLM Auger Spectra of 3d transition metals Z=23–26. *Journal of Electron Spectroscopy and Related Phenomena;* 82: 31–40.

4. Ursic, M, Kavcic, M, Budnar, M. 2003. Second order radiative contributions in the K□$_{1,3}$ X-ray spectra of 3d transition metals and their dependence on the chemical state of the element. *Nuclear Instruments and Methods in Physics Research B;* 211: 7–14.

5. Ito, Y, Tochio, T, Ohashi, H, Yamashita, M, Fukushima, S, Polasik, M, Slabkowska, K, Syrocki, L, Szymanska, E, Rzadkiewicz, J, Indelicato, P, Marques, J.P, Martins, M.C, Santos, J.P, Parente, F. 2016. K□$_{1,2}$ X-ray linewidths, asymmetry indices, and [KM] shake probabilities in elements Ca to Ge and comparison with theory for Ca, Ti and Ge. *Physical Review A;* 94: 042506.

6. Hölzer, G, Fritsch, M, Deutsch, M, Hartwig, J, Förster, E. 1997. K□$_{1,2}$andK□$_{1,3}$ X-ray emission lines of the 3d transition metals. *Physical Review A;* 56: 4554.

7. Ito, Y, Tochio, T, Oohashi, H, Vlaicu, A.M. 2006. Contribution of the [1s3d] shake process to K□$_{1,2}$ spectra in 3d elements. *Radiation Physics and Chemistry;* 75: 1534–1537.

8. Deutsch M,Hölzer G, Hartwig J, Wolf J, Fritsch M, Förster E, K□□and K□ X-ray emission spectra of copper, *Physical Review A* 1995,51, 283.

9. Sorum, H. 1987. The K□$_{1,2}$ X-ray spectra of the 3d transition metals Cr, Fe, Co, Ni and Cu. *Journal of Physics F: Metal Physics;* 17: 417–425.

10. Chantler, C.T, Kinnane, M.N, Su, C.-H, Kimpton, J.A. 2006. Characterization of K□ spectral profiles for vanadium, component redetermination for scandium, titanium, chromium, and manganese and development of satellite structure for Z=21 to Z=25. *Physical Review A*;73: 012508.

11. Chantler, C.T, Lowe, J.A, Grant, I.P. 2013. High accuracy reconstruction of titanium X-ray emission spectra, including relative intensities, asymmetry and satellites, and ab initio determination of shake magnitudes for transition metals. *Journal of Physics B: Atomic Molecular and Optical Physics;* 46: 015002.

12. Ito, Y, Tochio, T,Yamashita, M, Fukushima, S,Vlaicu, A.M, Syrocki, L, Slabkowska, K, Weder, E, Polasik, M, Sawicka, K, Indelicato, P, Marques, J.P, Sampaio, J.M, Guerra, M, Santos, J.P, Parente, F. 2018. Structure of high resolution K□$_{1,3}$ X-ray emission spectra for the elements from Ca to Ge. *Physical Review A***;** 97: 052505.

Celal Bayar University Journal of Science
Volume 15, Issue 1, 2019, p 57-64
Doi: 10.18466/cbayarfbe.459295

13. Limandri, S.P, Carreras, A.C, Bonetto, R.D, Trincavelli, J.C. 2010. K□□satellite and forbidden transitions in elements with 12≤Z≤30 induced by electron impact. *Physical Review A;* 81: 012504.

14. Weissmann, R, Koschatzky, R, Schnellhammer, W, Müller, K. 1977. Some Aspects of Auger Electron Spectra of 3d transition metal oxides. *Applied Physics;* 13: 43–46.

15. Aylikci, V, Kahoul, A, Kup Aylikci, N, Tirasoglu, E, Karahan, I.H. 2015. Empirical, semi-empirical and experimental determination of K X-ray fluorescence parameters of some elements in the atomic range 21≤Z≤30. *Spectroscopy Letters;* 48: 331–342.

16. Akman, F. 2016. Experimental values of K to Li sub-shell, K to L, and K to M shell vacancy transfer probabilities for some rare earth elements. *Applied Radiation and Isotopes;* 115: 295-303.

17. Scofield, J.H, Lawrence Livermore National Laboratory Report UCRL-51326 (1973).

18. Scofield, J.H. 1974. Relativistic Hartree-Slater Values for K and L X-Ray Emission Rates. *Atomic Data and Nuclear Data Tables;* 14: 121–137.

19. Krause, M.O., Oliver, J.H. 1979. Natural widths of atomic K and L levels, Kα X-ray lines and several KLL Auger lines. *J. Phys. Chem. Ref. Data; 8:* 329–338.

20. Perkins, S. T, Cullen, D. E, Chen, M. H, Hubbell, J.H, Rathkopf, J, Scofield, J.H. 1991. Tables and Graphs of Atomic Subshell Relaxation Data Derived from the LLNL Evaluated Atomic Data Library Z=1-100. *Lawrence Livermore National Laboratory Report; UCRL* 50400, vol. 30: Livermore.

21. Campbell, J.L, Papp, T. 2001. Widths of the atomic K–N7 levels. *Atomic Data and Nuclear Data Tables;* 77: 1–56.

22. Kup Aylikci, N, Tirasoglu, E, Karahan, I, Aylikci, V, Cengiz, E, Apaydin, G. 2010. Alloying effect on K shell X-ray fluorescence parameters and radiative Auger ratios of Co and Zn in ZnxCo1-x alloys. *Chemical Physics Letters*; 484: 368-373.

23. Kup Aylikci, N, Tirasoglu, E, Karahan, I, Aylikci, V, Eskil, M, Cengiz, E. 2010. Alloying effect on K X-ray intensity ratios, K X-ray production cross-sections and radiative Auger ratios in superalloys constitute from Al, Ni and Mo elements. *Chemical Physics;* 377: 100-108.

24. Cooper, J.N. 1944. Auger Transitions and Widths of X-Ray Energy Levels. *Physical Review;* 65: 155.